

# Evaluation of Dual Permeability of Gas Flow in Municipal Solid Waste: Experiment and Modeling

Lei Liu,<sup>a</sup> Qiang Xue,<sup>a</sup> Yong Wan,<sup>a</sup> and Yu Tian<sup>b</sup>

<sup>a</sup>State Key Laboratory of Geomechanics and Geotechnical Engineering, Institute of Rock and Soil Mechanics, Chinese Academy of Sciences, Wuhan 430071, China; lliu@whrsm.ac.cn, qiangx@whrsm.ac.cn (for correspondence)

<sup>b</sup>Wuhan Environment Investment & Development Co., Ltd, Wuhan 430019, China

Published online 29 June 2015 in Wiley Online Library (wileyonlinelibrary.com). DOI 10.1002/ep.12184

*Non-homogeneity of permeability largely depends on heterogeneity of the pore structure of waste in a landfill, which contributes to variation in gas flow state. Gas pressure dropping test (GPDT) was one of the most effective methods to describe the gas preferential flow, was used to investigate the gas breakthrough curves in initial pressures, moisture contents and degradation phases in lab test. Dual-permeability model was developed to quantify the gas preferential flow in waste column. The reliability of the model was verified by a good agreement from the gas flow rate between the simulation results and experimental results. The simulation results show the biodegradation of the waste produced an obviously decrease in the permeability in fracture system due to the variation of the particle distribution. The porosity and mass transfer in fracture system has largely decreased with the continued biodegradation and moisture content increasing. It will be provided useful evidence for assessing the gas preferential flow during the well operation in landfill. © 2015 American Institute of Chemical Engineers Environ Prog, 35: 41–47, 2016*

*Keywords:* dual permeability, waste, breakthrough curve, model, simulation

## INTRODUCTION

The capacity of the gas flow is one of the most important factors in evaluating gas emission and distribution in a landfill [1–3]. The variation of the gas flow rate depends on the distribution of the permeability and pore structure within the landfill.

Dual permeability model was developed, based on the assumption that the pore system was separated to two continue and connected between each other domains. For example, water flow in dual permeability model was presented using separate flow equations for the fracture and matrix pore systems [4]. The spatial variability of the permeability in pore system was simplified by using this assumption, to simulate the water or gas movement under preferential flow effect [5–7].

Stochastic models have also been applied to predict preferential flow in different soils [8]. The stochastic simulation could be simplified by implanting the probability density functions (PDFs) [9,10]. Besson *et al.* [11] presented the simulation of dominant transport identified as being a stochastic-convective process in a loamy soil. The quantification of

PDFs will be still a choke point to further apply the stochastic models for the evaluation of the preferential flow.

The distribution of the constituents of the waste is inhomogeneous, resulting in strong heterogeneity of the waste body structure. Particle and pore size as well as shapes and solid material types vary [12,13]. As the penetration performance is closely related to pore structure, the permeability of the waste body is also heterogeneous in the landfill [14–16]. Han *et al.* [17] found that the preferential flow was still obviously occurred in column composed by uniform paper at 4-cm scale based on the water flow rate measurement.

Some researchers attempted to describe the preferential flow in the waste body by using the dual permeability or dual porosity model [18–20]. Rosqvist *et al.* [21] studied leachate transport in waste by model interpretation of experimental break-through curves, found the preferential flow continued in long-term. The reliability of the dual permeability model should be verified by comparison flow rate between the test and simulation. The measurement of the breakthrough curves was an effective method for quantification assessing the preferential flow, provided the data for inverting the relative parameters in dual permeability model, including outflow rate or solute concentration.

This method has been reported in some literatures for the simulation of liquid BTCs in some scenes [13,17,22]. In recent years, the measurement of the gas BTCs was conducted in tracer tests in lab-scale [23,24]. With the preceding analysis, the suitability of the dual media theory to access the gas flow in the waste body should be discussed using test and model simulations.

Previous studies often defined permeability based on one constant to simplify the simulation of gas flow in landfill. The gas pressure and flow rate were determined by the single permeability model [1,3,25–27]. The long-term field monitoring test suggested that the simulation results of the flow rate from gas wells were inaccurate, adding the deviation of the collection volume in wells [3].

The permeability was recorded if the external gas flow rate became stable under pressure difference in the gas seepage test. As a result of the non-uniformity of the waste constituents, a portion of the gas flows out through the macro-domain first, followed by another portion flowing out through the micro-domain mainly because of the significant difference in seepage capacity between the macro- and micro-domains [17]. It is critical to monitor the gas flow across the waste body and develop the mathematical model

**Table 1.** Characteristics of fresh and degraded MSW sample.

Reactor	Degradation-phase (day)	Initial pressure (MPa)	Sample mass (kg)	Moisture content (%)
A1	0	0.1	1.127	25.0
A2	0	0.05	1.127	25.1
A3	0	0.02	1.127	24.9
B1	0	0.1	1.127	25.0
B2	0	0.1	1.303	35.0
B3	0	0.1	1.579	45.0
C1	0	0.1	1.238	25.0
C2	30	0.1	1.174	24.7
C3	60	0.1	1.116	24.5

for evaluation the seepage capacity in the two domains. However, no methods have been conducted to characterize the gas preferential flow in waste sample by model or test.

The objectives of this study are (1) to develop the dual-permeability model of gas flow to describe the preferential flow through the waste body; (2) to predict the permeability and porosity in the two domains based on breakthrough curves (BTCs); (3) to compare the test results in lab-scale with the simulation results of the outflow rate to estimate the reliability of the dual-permeability model.

#### MATERIALS AND METHODS

##### Materials

To improve the seepage effect, we ensured that the maximum quantity of the waste sample was <4 cm by artificial screen from fresh waste. The sample consisted of 50% food was represented by 40% vegetable waste and 10% meat, 15% paper was represented by shredded paper, 3% textile was represented by shredded clothing, 3% plastic was represented by shredded sack, 3% wood was represented by branch, 6% glass was represented by yard waste, and 20% soil. A1, A2, and A3 were prepared with three initial pressures. B1, B2, and B3 simulated the moisture contents. C1, C2, and C3 were conducted at degradation phases. The parameters are shown in Table 1.

##### Porosity-Permeability Test Experiment

The test experiment selected the porosity-permeability measurement system designed by the author. This system consisted of a loading piston, a sample pressure chamber (SPC), a standard chamber (SC), a nitrogen bottle, gas flow meter (D07, Beijing Sevenstar, China) and analysis of data collected system. The waste sample scale in the SPC was 100 mm × 350 mm (shown in Figure 1).

##### Gas Pressure Dropping Test

The BTCs were obtained by gas pressure dropping test, which involved the following steps: (1) closing the SPC, (2) inflating the nitrogen into the SC to increase the gas pressure to a certain value, (3) opening the export and input valves in the SPC to record the outflow rate from the export valve of the SPC and the gas pressure in SC. The dropping process of the gas pressure in the SC could be addressed in the boundary condition at the input of the SPC. The gas pressure was monitored by pressure sensors (DG-010, Guangzhou Senex, China).

##### Bio-Degradation Operation

The mixed waste was placed in the SPC, serve as the reactor of bio-degradation. The SPC was a hermetical stainless steel (316L) column, could be used to conduct the

anaerobic condition for waste degradation. The SPC was placed in a lab-chamber retained temperature at 33–35°C which could provide a relative appropriate environment for organic degradation. The gas produced in reactor was collected by bag. Bio-degradation process was recorded by measuring the organic content. Organic content and Particle size distribution of waste sample was determined by standard procedure (MOHURD CJJ/T 204-2013; [28]).

##### Porosity-Permeability Measurement

The total permeability was available by constant pressure test. The gas pressure in inlet was measured by pressure sensors. The pressure set up atmosphere. The gas flow rate in export was recorded by flow meter, when it was to steady.

The gas through the waste medium is performed by the Darcy law [29]:

$$k = \frac{2P_B Q_B \mu L}{A(P_A^2 - P_B^2)} \quad (1)$$

Where  $k$  is permeability;  $Q_B$  is gas flow rate in export;  $\mu$  is gas viscosity coefficient;  $P_A$  is gas pressure in inlet;  $P_B$  is gas pressure in export;  $L$  is sample length;  $A$  is sample sectional area.

The total porosity measured in this system, based on the Boyle-Mariotte relation. The detail information of the test step was preserved in Stoltz *et al.*, [30].

The relation is given as follow,

$$V_{SC} \cdot P_1 = (V_{SPC} - V_s + V_{SC}) \cdot P_2 \quad (2)$$

Where,  $V_{SC}$  is the volume of SC,  $V_{SPC}$  is the volume of SPC,  $V_s$  is the volume of solid sample,  $P_1$  is the initial gas pressure in SC,  $P_2$  is the steady gas pressure across the SPC and SC.

$$\Phi_t = \frac{V_{SPC} - V_s}{V_{SPC}} \quad (3)$$

Where,  $\Phi_t$  is the total porosity.

##### DUAL-PERMEABILITY MODEL OF GAS FLOW

Dual-permeability model describe gas flow in the fracture and matrix pore system, using two equations to represent gas flow state in the two domains [6,31]:

$$\frac{\partial}{\partial t} (\rho_f \Phi_f) = \nabla \cdot \left( \rho_f \frac{k_f}{\mu} \cdot \nabla (P_f) \right) + Q_{mf} \quad (4)$$

$$\frac{\partial}{\partial t} (\rho_m \Phi_m) = \nabla \cdot \left( \rho_m \frac{k_m}{\mu} \cdot \nabla (P_m) \right) - Q_{mf} \quad (5)$$

Where the subscript “ $f$ ” defines a property of the fracture pore system, the subscript “ $m$ ” represents the matrix,  $\Phi_f$  and  $\Phi_m$  is the porosity in fracture and matrix domain, respectively.  $\rho_f$  and  $\rho_m$  is gas density in fracture and matrix domain, respectively, assumed following the ideal gas law.  $\mu$  is coefficient of viscosity,  $k_f$  and  $k_m$  is the permeability in fracture and matrix domain, respectively. The total permeability is described by:

$$k_t = w_f \cdot k_f + (1 - w_f) \cdot k_m \quad (6)$$

Where  $w_f$  is the relative volumetric proportion of the fracture pore system ( $0 < w_f < 1$ ). The relationship between the total porosity and porosity in two domains could be written by [4]:

$$\Phi_t = w_f \cdot \Phi_f + (1 - w_f) \cdot \Phi_m \quad (7)$$

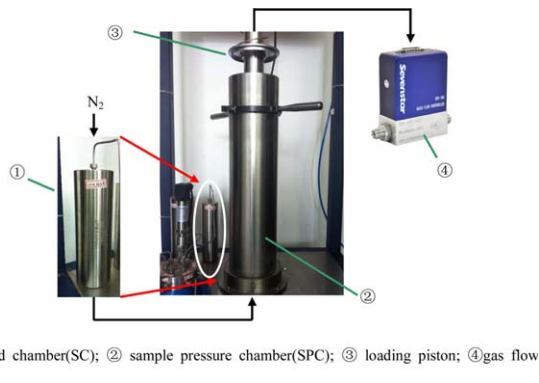


**Figure 1.** Schematic of the Test experiment. [Color figure can be viewed in the online issue, which is available at [wileyonlinelibrary.com](http://wileyonlinelibrary.com).]

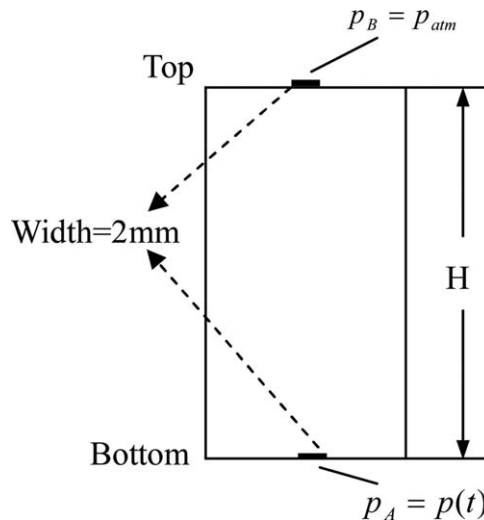


**Figure 2.** Profile of the simulation model.

Where  $Q_{mf}$  is the gas transfer term, can be described as

$$Q_{mf} = \alpha_f \cdot \delta \frac{\rho k_m}{\mu} (P_m - P_f) \quad (8)$$

Where  $\delta$  is the shape factor, developed by Zimmerman [32].  $\alpha_f$  is the mass transfer coefficient, depended largely on the pore structure and preferential flow pathway [7]. The gas transfer term is ignored in the single-permeability model, which have “one” permeability and “one” porosity.

The dual-permeability model could be used to estimate the process of the gas throughout the waste sample, including permeability and porosity in two-domain, based on the dropping test. The first-type boundary condition was employed in the inlet and outlet at the column for these simulations. The parameters in dual-permeability model were determined by using optimization routine [shown in Ref. 3] with the data of gas flow rate from experiments. The numerical simulation program was completed by using Matlab language.

The initial height of the simulation model,  $H$ , is 350 mm. The top port and bottom of the SPC was connected by bore size 2 mm conduit. Then the width of the pressure boundary in the ports was 2 mm (see Figure 2). The gas flow rate in the outlet of SPC is a process which varied with time after the valve in inlet opened connected with SC. So, the boundary condition in inlet was simplified to gas pressure boundary. The gas pressure in inlet was recorded, known as  $p(t)$ . The pressure boundary of the outlet in SPC was simplified to atmosphere. The initial gas pressure in SPC was also atmosphere. The height of the simulation model was 289, 269, and 257 mm, respectively, in simulation cases of fresh waste and 30 and 60 days degradation waste.

## EXPERIMENTAL RESULTS

### BTCs Affected by Initial Pressure

The gas pressure was from 100 to 2000 Pa during landfill operation. If the gas was discharged at a low degree, the gas pressure could reach from 2490 to 9500 Pa [33]. Therefore, 0.1, 0.05, and 0.02 MPa were selected as the initial pressures in A1, A2, and A3 to conduct the seepage tests.

The variation of BTCs exhibited a similar trend. The peak of the outflow rate and the cross-time rose as the initial pressure increased (Figure 3).

### BTCs Affected by Moisture Content

Figure 4 shows the BTCs distribution in the moisture content. The total permeability and total porosity were eliminated as the moisture content decreased (see Table 2), increasing the curve amplitude and the peak, as well as reducing the cross-time. This

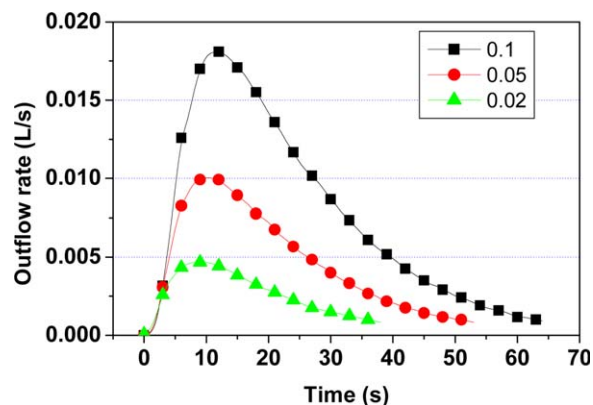


**Figure 3.** The breakthrough curves distribution in initial pressures. [Color figure can be viewed in the online issue, which is available at [wileyonlinelibrary.com](http://wileyonlinelibrary.com).]

condition occurred because most pore spaces were occupied when the moisture content increased, raising the permeability ratio between the fracture and matrix system, resulting in significantly increased gas flow through the fracture system and adding to the peak of the outflow rate. Therefore, the variation of the gas flow rate was related to the total permeability and porosity. The permeability and porosity in the two domains should be considered.

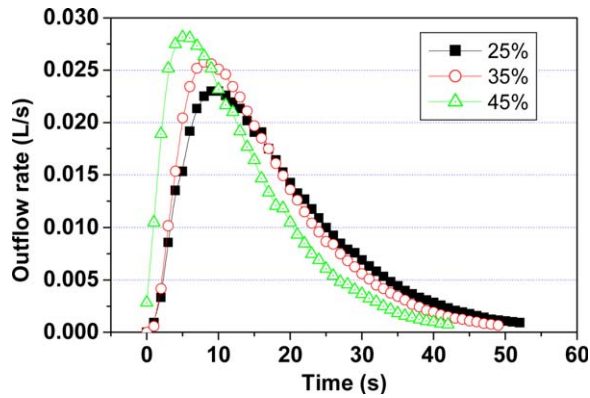
### BTCs Affected by Degradation

Figure 5 shows the 30- and 60-day degradations of the test and simulation results of BTCs in the fresh sample. The simulation results of the outflow rate distribution were consistent with the test results, suggesting that the dual-permeability model could be used to represent the gas flow across the pore system. The test results indicated that the peak of the outflow rate declined with the degradation of the waste sample. As the waste particle became more compact after material decomposition, the strain of the sample also increased, resulting in a reduction in permeability and porosity (Table 3).

## SIMULATION RESULTS

### The Variation of BTCs with Permeability Ratio and Volumetric Proportion

Figure 6 shows the simulation results about BTCs in different permeability ratios. The peak of the BTCs increased,



**Figure 4.** The breakthrough curves distribution in moisture contents. [Color figure can be viewed in the online issue, which is available at [wileyonlinelibrary.com](http://wileyonlinelibrary.com).]

**Table 2.** The total permeability and porosity test results with moisture contents.

Moisture content (%)	Permeability ( $10^{-11} \text{ m}^{-2}$ )	Porosity (%)
25%	0.793	0.463
35%	0.720	0.421
45%	0.672	0.373

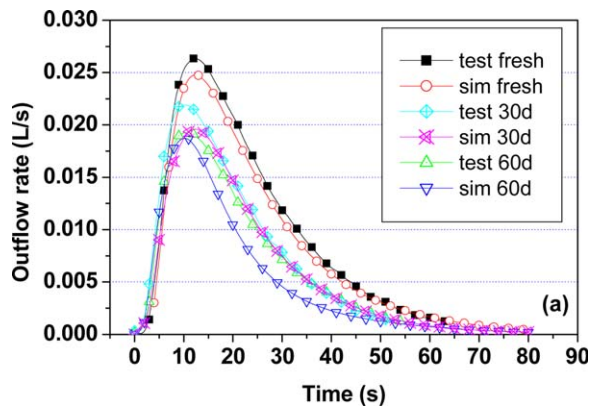


**Figure 5.** The breakthrough curves distribution in degradation phases, monitoring results and simulation results from dual-permeability model. [Color figure can be viewed in the online issue, which is available at [wileyonlinelibrary.com](http://wileyonlinelibrary.com).]

**Table 3.** Test results in degradation phases.

Cells	Loading (MPa)	Total permeability ( $10^{-11} \text{ m}^{-2}$ )	Total porosity (%)	Strain (%)	Organic content (%)
Fresh	0.05	1.02	0.559	17.3	83.5
30d	0.05	0.785	0.514	23.1	55.1
60d	0.05	0.650	0.486	26.5	22.6

dropping the cross-time as the permeability ratio increased. The permeability was increased after the permeability ratio was raised, accelerating the gas velocity through the fracture system and reducing the cross-time.

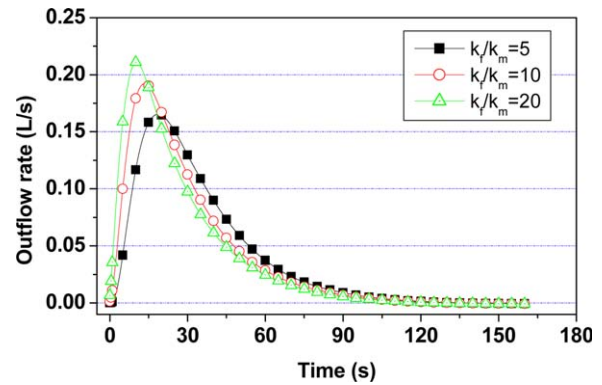


**Figure 6.** Gas outflow rate in permeability ratios. [Color figure can be viewed in the online issue, which is available at [wileyonlinelibrary.com](http://wileyonlinelibrary.com).]

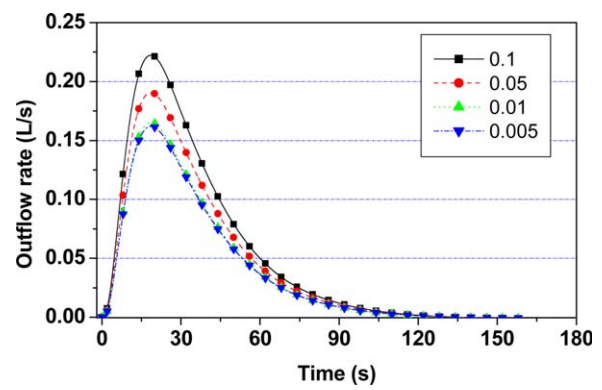


**Figure 7.** Gas outflow rate in relative volumetric proportions. [Color figure can be viewed in the online issue, which is available at [wileyonlinelibrary.com](http://wileyonlinelibrary.com).]

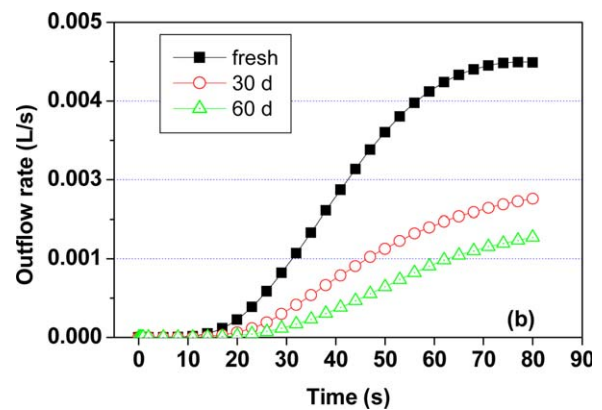


**Figure 8.** The simulation results of breakthrough curve from single-permeability model. [Color figure can be viewed in the online issue, which is available at [wileyonlinelibrary.com](http://wileyonlinelibrary.com).]

Figure 7 illustrates the simulation results about BTCs in different  $w_f$ . As the  $w_f$  was eliminated, the fraction of the fracture in the entire pore system decreased, resulting in the reduction of seepage capacity in the fracture domain as well as the gas outflow rate.

**Table 4.** The inversion data of the permeability and porosity with degradation.

Cells	$k_f$ ( $10^{-11} \text{ m}^{-2}$ )	$k_m$ ( $10^{-11} \text{ m}^{-2}$ )	$k_f/k_m$	$\phi_f$	$\phi_m$	$\phi_f/\phi_m$	$\alpha_f$
Fresh	3.25	0.77	4.22	0.10	0.61	0.16	0.05
30d	2.15	0.70	3.07	0.08	0.56	0.14	0.02
60d	1.41	0.565	2.49	0.03	0.54	0.05	0.006

**Table 5.** The inversion data of the permeability and porosity with moisture contents.

Moisture content	$k_f$ ( $10^{-11} \text{ m}^{-2}$ )	$k_m$ ( $10^{-11} \text{ m}^{-2}$ )	$k_f/k_m$	$\phi_f$	$\phi_m$	$\phi_f/\phi_m$	$\alpha_f$
25%	2.35	0.62	3.79	0.062	0.51	0.12	1.0
35%	2.38	0.54	4.41	0.041	0.46	0.09	0.31
45%	2.41	0.48	5.02	0.033	0.41	0.08	0.08

**Comparison of Dual-Permeability and Single Models**

The dual-permeability model and single-permeability model were used to predict the gas flow in waste sample, to estimate the reliability of the models. The total permeability and total porosity were adopted from the lab test, shown in Table 3.

Figure 8 shows the BTCs simulated by the single-permeability model in the degradation phases. The simulation results showed that the gas outflow rate from the input to the output could not be represented by the single-permeability model. This model was proposed based on the assumption of uniformity in permeability. The model could not show the flow process in the initial phase in which the gas flows out of the fracture system in the practical waste sample (see Figure 5). The outflow rate value from the single-permeability model was significantly lower than that in the monitored results, and the breaking time was considerably longer than that in the monitored results.

**DISCUSSION**

**The Permeability Ratio  $k_f/k_m$  with Moisture Content**

$k_f/k_m$  is the key parameter to predict the gas movement under the preferential flow effect. The  $k_f/k_m$  available from the inversion of test data presented a decrease with the increasing of the water content (see Table 5). The inversion result was agreed with the simulation results from the BTCs in Figure 6. It could verify the reliability of the inversion permeability in two domains based on the BTCs.

**Permeability and Porosity in Two Domains with Degradation**

The optimized parameters were given by numerical inversion as shown in Table 4. The permeability ratio  $k_f/k_m$  in the fresh sample was slightly higher than that in the decomposed sample. This indicated that the relative predominance of the permeability capacity in fracture system was eliminated. The decreasing of the permeability and porosity in fracture system during degradation process was higher than which in matrix system. This indicated that the degradable constituents broken into smaller particles in the whole degradation phases [34], leading to reduction of the pore space in fracture system. The particle size had an obviously reduction during degradation phase (Figure 9). This result was agreed with the test from Reddy *et al.* [35] of the artificial waste material.

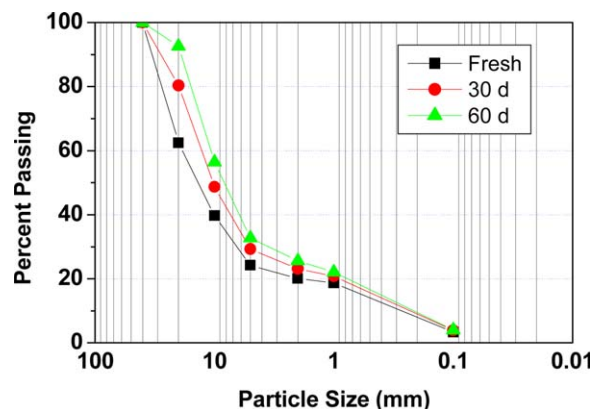


**Figure 9.** Particle size distribution of waste sample at different phase of degradation. [Color figure can be viewed in the online issue, which is available at [wileyonlinelibrary.com](http://wileyonlinelibrary.com).]

**Permeability and Porosity in Two Domains with Moisture Contents**

The inversion data of the permeability and porosity with moisture contents were given in Table 5. There was a decrease in  $\phi_f$  and non-obvious variation in  $k_f$  with the increasing of the water content. As the water added, the  $\phi_m$  and  $k_m$  were decreased. It suggested that the non-flow space in fracture system was occupied with the spare water, resulting minor effect in effective flow space in preferential pathways.

**Modification of Gas Transfer Term**

According to the simulation result, the mass transfer coefficient was influenced by the variation of the pore structure as a result of organic degradation and the variation of the water content (shown in Tables 4 and 5). The gas transfer term should be amended, as the variation of the connectivity between the fracture and matrix systems in waste sample.

**CONCLUSIONS**

A laboratory test of the capacity of the gas passing through the waste sample was conducted. The dual-permeability model of the gas flow was developed to predict

the gas preferential flow in the waste sample. The conclusions are as follows:

1. A typical heterogeneous property of gas flow occurred in the waste body. The fraction of the space in the fracture and matrix systems was dependent on the distribution of the pore structure. The pore structure had a direct effect on the gas flow state.
2. The single-permeability model could not simulate the gas breakthrough process. The BTCs represented by the dual-permeability model were consistent with the curves from the test. The feasibility and the reliability of the prediction method of parameters from the dual-permeability model was verified.
3. The particle distribution was modified by the biodegradation of the decomposing material in the waste sample, which led to the variation in the connectivity between the two domains, especially resulting larger contribution on the permeability in fracture system. The parameter amendment in mass transfer was needed, when the pore structure of the waste was changed due to continued biodegradation and moisture content increasing.

#### ACKNOWLEDGMENTS

This research was supported by the National Basic Research Program of China (973 Program) (2012CB719802); the Special Fund for Basic Research on Scientific Instruments of the National Natural Science Foundation of China (51209197, 51279199); disciplinary Collaborative Teams Program for Science, Technology and Innovation, Chinese Academy of Sciences.

#### LITERATURE CITED

1. Nastev, M., Therrien, R., Lefebvre, R., & Gélinas, P. (2001). Gas production and migration in landfills and geological materials, *Journal of Contaminant Hydrology*, 52, 187–211.
2. Liu, L., Liang, B., Xue, Q., Zhao, Y., & Yang, C. (2011). The modelling of biochemical-thermal coupling effect on gas generation and transport in MSW landfill, *International Journal of Environment and Pollution*, 46, 216–229.
3. Xue, Q. & Liu, L. (2014). Study on optimizing evaluation and recovery efficiency for landfill gas energy collection., *Environmental Progress & Sustainable Energy* 33, 1419, 1424.
4. Vogel, T., Gerke, H.H., Zhang, R., & Van Genuchten, M.T. (2000). Modeling flow and transport in a two-dimensional dual-permeability system with spatially variable hydraulic properties, *Journal of Hydrology*, 238, 78–89.
5. Köhne, J.M., Köhne, S., & Šimůnek, J. (2009). A review of model applications for structured soils: a water flow and tracer transport, *Journal of Contaminant Hydrology* 104, 4–35.
6. Nie, R.S., Meng, Y.F., Jia, Y.L., Zhang, F.X., Yang, X.T., & Niu, X.N. (2012). Dual porosity and dual permeability modeling of horizontal well in naturally fractured reservoir, *Transport in Porous Media*, 92, 213–235.
7. Wang, Y., Bradford, S.A., & Šimůnek, J. (2014). Estimation and upscaling of dual-permeability model parameters for the transport of *E. coli* D21g in soils with preferential flow, *Journal of Contaminant Hydrology*, 159, 57–66.
8. Chris, B.G. & Henry, L. (2012). Chapter 18—Subsurface flow networks at the Hillslope scale. *Detection and Modeling Hydrogeology*, 559–593.
9. Dagan, G. (1993). Higher-order correction of lognormal conductivity of heterogeneous formations of lognormal conductivity distribution, *Transport Porous Media*, 12, 279–290.
10. Gautier, Y. & Noetinger, B. (1997). Preferential flow-paths detection for heterogeneous reservoirs using a new renormalization technique, *Transport in Porous Media*, 26, 1–23.
11. Besson, A., Javaux, M., Bièdiers, C.L., & Vancloostera, M. (2011). Impact of tillage on solute transport in a loamy soil from leaching experiments, *Soil & Tillage Research* 112, 47–57.
12. Beaven, R.P., Powrie, W., & Zardava, K. (2011). Hydraulic properties of MSW. *Geotechnical Characterization, Field Measurement, and Laboratory Testing of Municipal Solid Waste*, 1–43. doi: 10.1061/41146(395)1
13. Woodman, N.D., Siddiqui, A.A., Powrie, W., Stringfellow, A., Beaven, R.P., & Richards, D.J. (2013). Quantifying the effect of settlement and gas on solute flow and transport through treated municipal solid waste, *Journal of Contaminant Hydrology*, 153, 106–121.
14. Capelo, J. & De Castro, M. (2007). Measuring transient water flow in unsaturated municipal solid waste—A new experimental approach, *Waste Management*, 27, 811–819.
15. Jung, Y., Imhoff, P.I., & Stefan, F. (2011). Estimation of landfill gas generation rate and gas permeability field of refuse using inverse modeling, *Transport in Porous Media*, 90, 41–58.
16. Tinetti, A.J., Oxarango, L., Bayard, R., Benbelkacem, H., Stoltz, G., Staub, M.J., & Gourc, J.P. (2011). Experimental and theoretical assessment of the multi-domain flow behaviour in a waste body during leachate infiltration, *Waste Management*, 31, 1797–1806.
17. Han, B., Scicchitano, V., & Imhoff, P.T. (2011). Measuring fluid flow properties of waste and assessing alternative conceptual models of pore structure, *Waste Management*, 31, 445–456.
18. Rosqvist, H. & Destouni, G. (2000). Solute transport through preferential pathways in municipal solid waste, *Journal of Contaminant Hydrology*, 46, 39–60.
19. McCreanor, P. & Reinhart, D. (2000). Mathematical modeling of leachate routing in a leachate recirculating landfill, *Water Research*, 34, 1285–1295.
20. Beaven, R., Barker, J.A., & Hudson, A. (2003). Description of a tracer test through waste and application of a double porosity model. In: *Proceeding Sardinia 2003, 9th International Waste Management and Landfill Symposium*. Santa Margherita di Pula, Cagliari, Italy.
21. Rosqvist, N.H., Dollar, L.H., & Fourie, A.B. (2005). Preferential flow in municipal solid waste and implications for long-term leachate quality: valuation of laboratory-scale experiments, *Waste Management Research*, 23, 367–380.
22. Woodman, N.D., Rees-White, T.C., Stringfellow, A.M., Beaven, R.P., & Hudson, A.P. (2015). Multiple-tracer tests for contaminant transport process identification in saturated municipal solid waste, *Waste Management*, 38, 250–262.
23. Jung, Y., Imhoff, P.I., Augenstein, D., & Yazdani, R. (2011). Mitigating methane emissions and air intrusion in heterogeneous landfills with a high permeability layer. *Waste Management*, 31, 1049–1058.
24. Woodman, N.D., Rees-White, T.C., Stringfellow, A.M., Beaven, R.P., & Hudson, A.P. (2014). Investigating the effect of compression on solute transport through degrading municipal solid waste, *Waste Management*, 34, 2196–2208.
25. Vigneault, H., Lefebvre, R., & Nastev, M. (2004). Numerical simulation of the radius of influence for landfill gas wells, *Vadose Zone Journal*, 3, 909–916.
26. Sanchez, R., Hashemi, M., Tsotsis, T.T., & Sahimi, M. (2006). Computer simulation of gas generation and transport in landfills—ii: Dynamic conditions, *Chemical Engineering Science*, 61, 4750–4761.
27. Garg, A. & Achari, G. (2010). A comprehensive numerical model simulating gas, heat, and moisture transport in

- sanitary landfills and methane oxidation in final covers, *Environmental Modeling & Assessment*, 15, 397–410.
28. Ministry of Housing and Urban-Rural Development of the People's Republic of China (MOHURD), (2014), Technical specification for soil test of landfilled municipal solid waste (CJJ/T 204-2013). China Architecture & Building Press, China.
  29. Ye, W., Wang, C., Wang, Q., & Chen, B. (2009), Laboratory tests on the characteristics of air-permeation in unsaturated Shanghai soft soil, *Journal of Engineering Geology (in Chinese)*, 17, 244–248.
  30. Stoltz, G., Gourc, J., & Oxarango, L. (2010). Liquid and gas permeabilities of unsaturated municipal solid waste under compression, *Journal of Contaminant Hydrology*, 118, 27–42.
  31. Köhne, J.M.M. & Simunek, B.P.J. (2006). Inverse dual-permeability modeling of preferential water flow in a soil column and implications for field-scale solute transport., *Vadose Zone Journal*, 5, 59–76.
  32. Zimmerman, R.W., Hadgu, T., & Bodvarsson, G.S. (1996). A new lumped-parameter model for flow in unsaturated dual-porosity media, *Advances in Water Resources*, 19, 317–327.
  33. McBean, E.A., Rovers, F.A., & Farquhar, G.J. (1995). *Solid waste landfill engineering and design* (pp. 390–391), Englewood Cliffs, NJ: Prentice Hall PTR.
  34. Hossain, M.S., Penmethsa, K.K., & Hoyos, L. (2009). Permeability of municipal solid waste in bioreactor landfill with degradation, *Geotechnical and Geological Engineering*, 27, 43–51.
  35. Reddy, K.R., Hettiarachchi, H., Gangathulasi, J., & Bogner, J.E. (2011). Geotechnical properties of municipal solid waste at different phases of biodegradation, *Waste Management*, 31, 2275–2286.
-